Electronic Supplementary Material (ESI) for Materials Chemistry Frontiers.

Supporting Information

Triazine based polyimide framework derived N-doped porous carbons: a study of their capacitive behaviour in aqueous acidic electrolyte

Namrata Deka,[a] Rajesh Patidar,[b] S. Kasthuri,[c] N. Venkatramaiah[c] and Gitish K. Dutta[a*]*

[a] Department of Chemistry, National Institute of Technology Meghalaya, Bijni complex, Laitumkhrah, Shillong-793003, Meghalaya, India

[b] Analytical and Environmental Science Division & Centralized Instrument Facility, CSIR-Central Salt & Marine Chemicals Research Institute, Bhavnagar-364002, Gujarat, India

[c] Department of Chemistry, SRM Institute of Science and Technology (SRMIST), Chennai-603203, Tamil Nadu, India

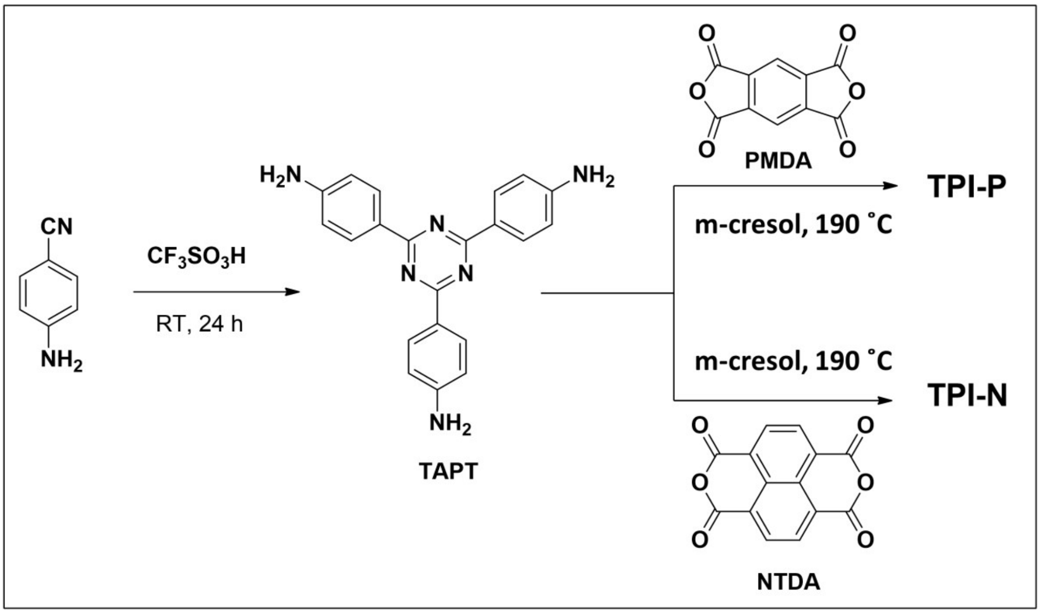

Scheme S1 Synthesis of TPI based porous organic frameworks, TPI-P and TPI-N.

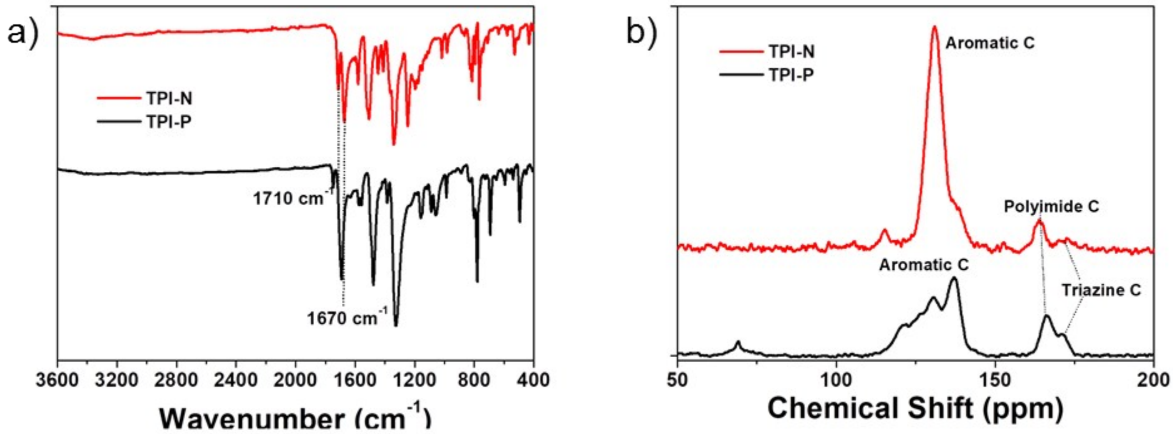

Fig. S1 a) FT-IR spectra of TPI-P/TPI-N frameworks; b) ^{13}C CP-MAS NMR spectra of TPI-P/TPI-N frameworks.

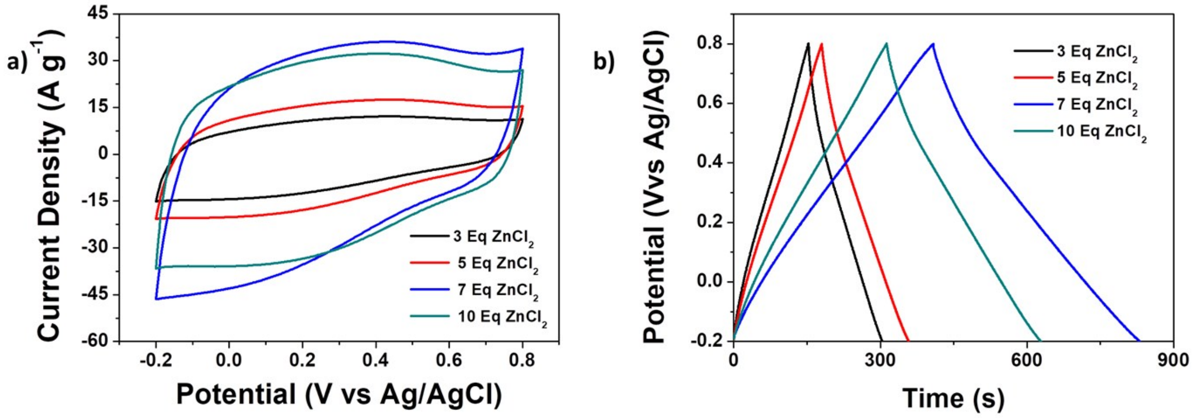

Fig. S2 CV and GCD curves of TPI-P-700 using different equivalents of $ZnCl_2$ in three electrode system.

Table S1 Electrochemical performance of N-doped porous carbon synthesized by using different amounts of $ZnCl_2$

Precursor	$ZnCl_2$ equivalent	S_{BET} (m^2 g^{-1})	Temperature (ºC)	C_s (F g^{-1})[a]	Electrolyte	Potential Range (V)
TPI-P	3	448	700	150	1 M H_2SO_4	-0.2 to 0.8
TPI-P	5	972	700	200	1 M H_2SO_4	-0.2 to 0.8
TPI-P	7	1650	700	423	1 M H_2SO_4	-0.2 to 0.8
TPI-P	10	1226	700	320	1 M H_2SO_4	-0.2 to 0.8

[a] calculated from GCD curves in three electrode system.

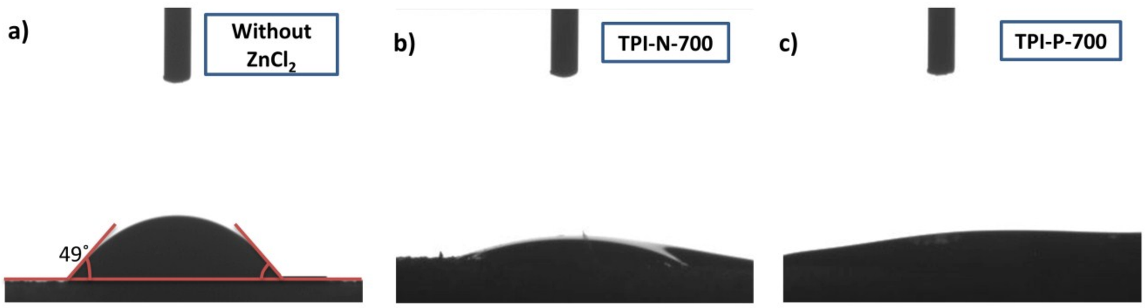

Fig. S3 Water contact angle images of a) TPI-P carbonized without $ZnCl_2$; b) TPI-N-700; c) TPI-P-700.

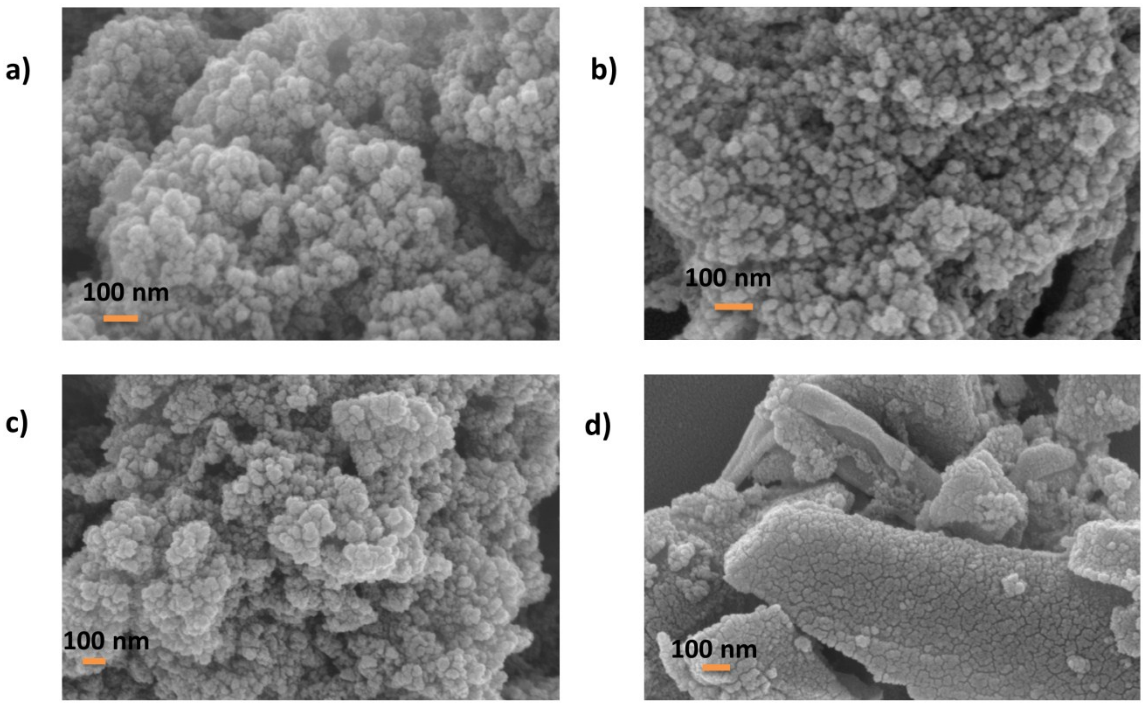

Fig. S4 FE-SEM images of a) TPI-P framework; b) TPI-N framework; c) TPI-P carbonized without $ZnCl_2$; d) TPI-P-700.

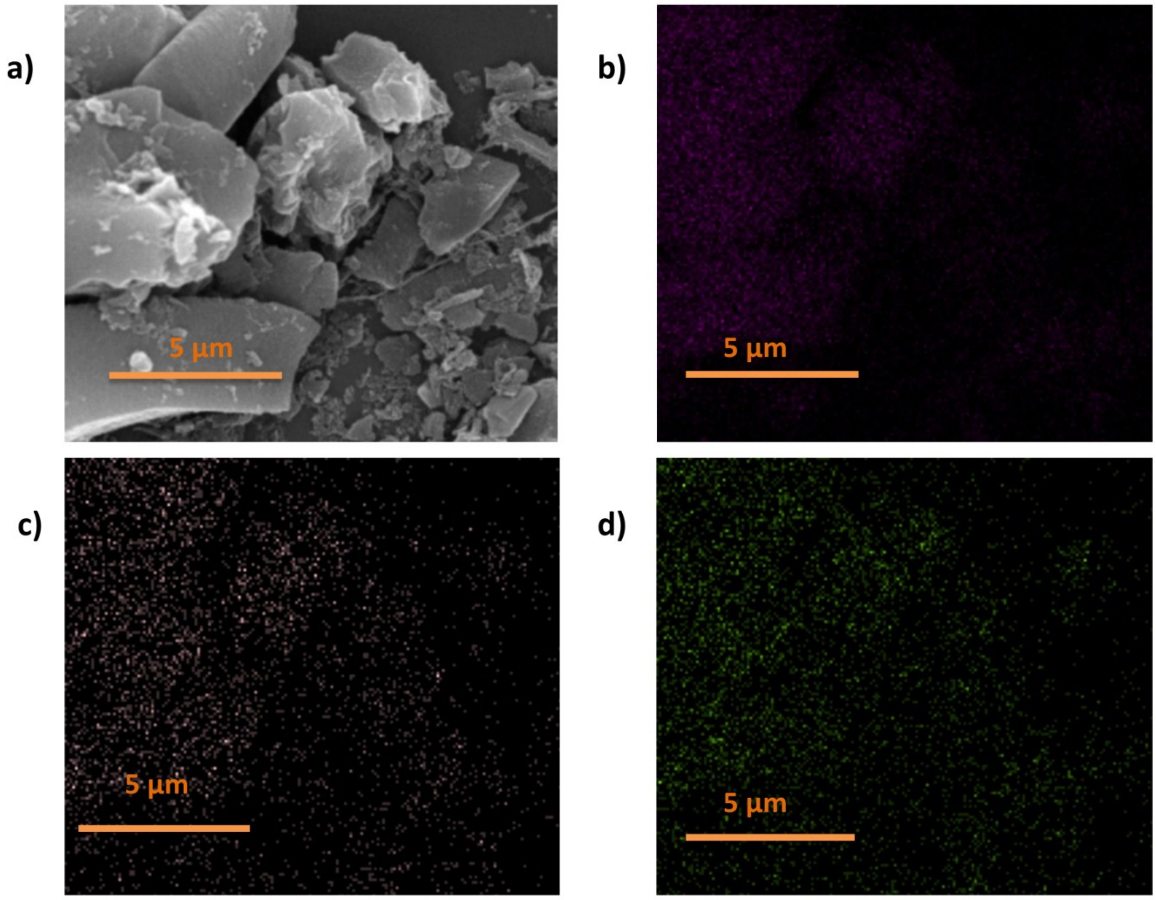

Fig. S5 a) FE-SEM image of TPI-P-700 and representative elemental mapping of b) carbon (purple); c) nitrogen (light pink); d) oxygen (green) elements.

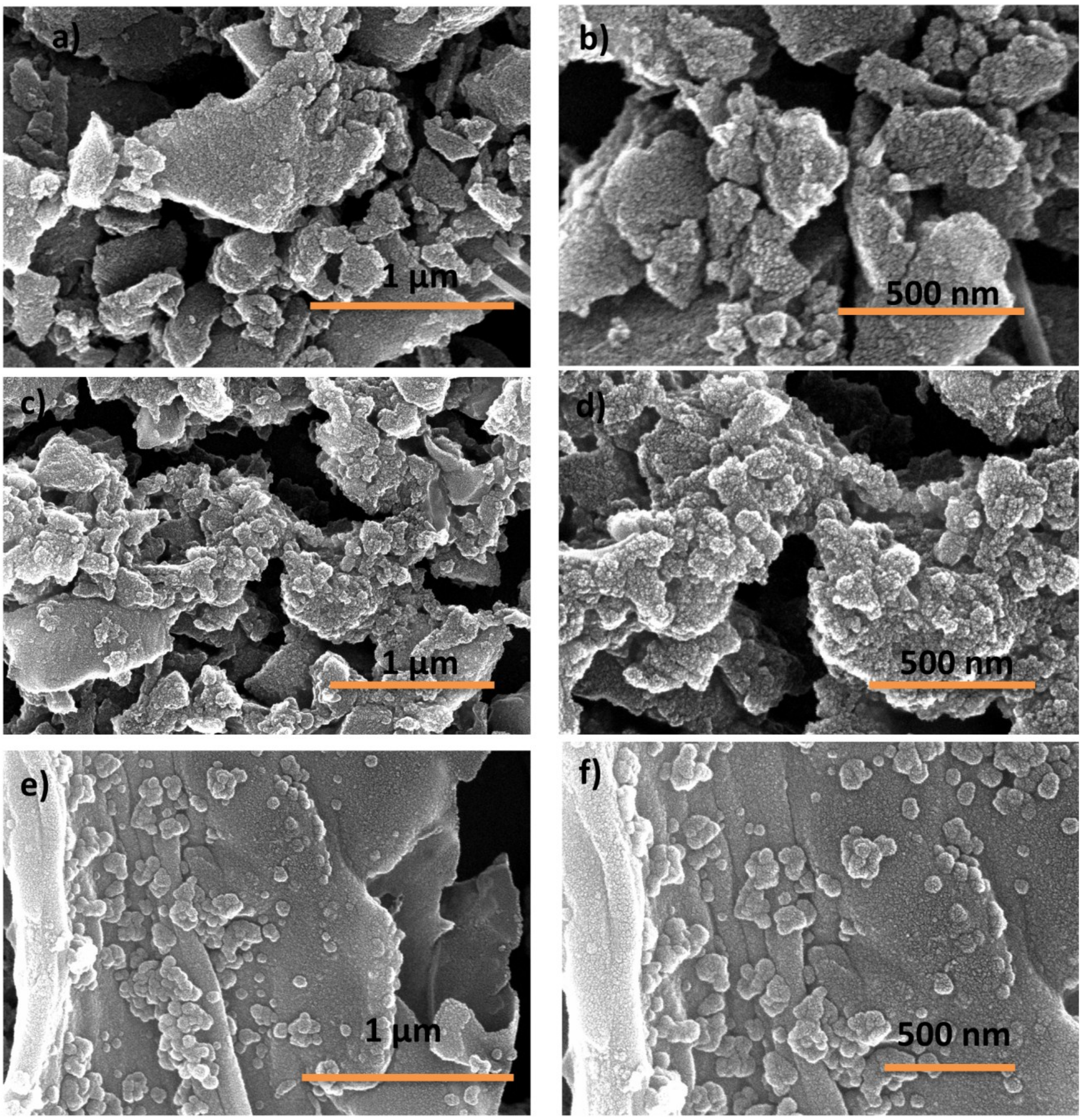

Fig. S6 FE-SEM images of (a, b) TPI-P-600; (c, d) TPI-N-600; (e, f) TPI-N-700.

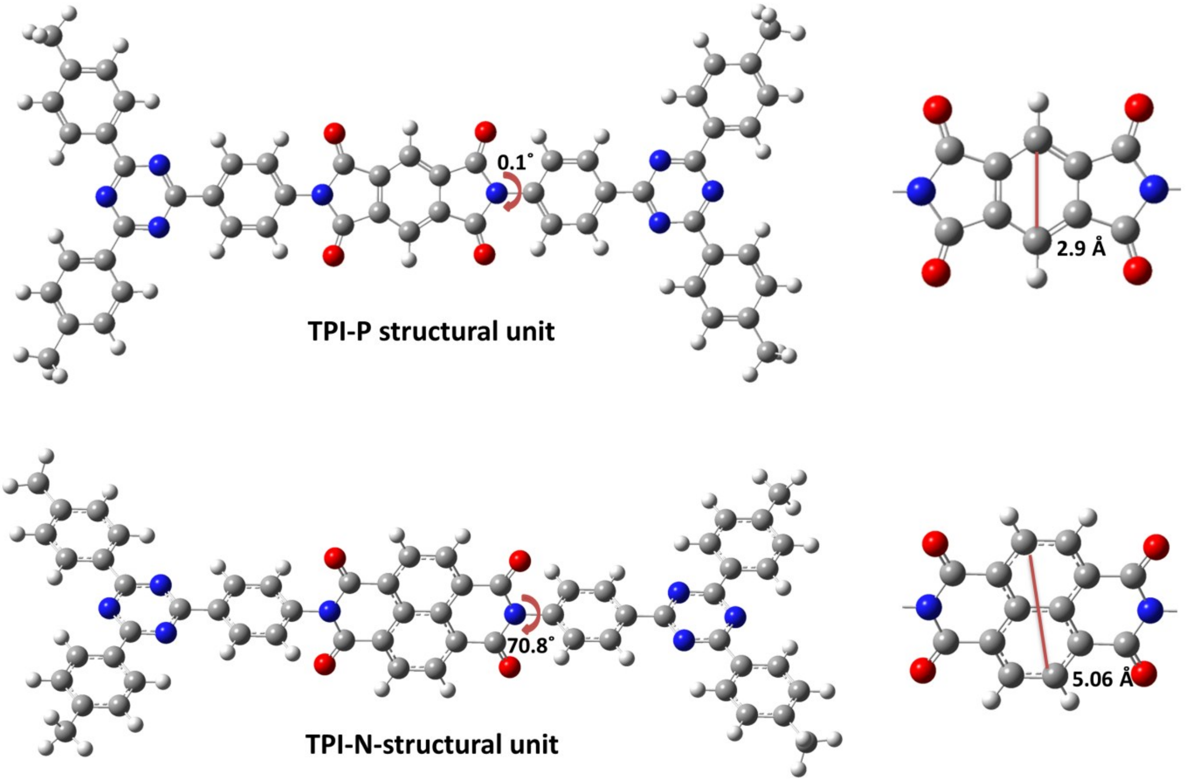

Fig. S7 DFT optimized geometry of TPI-P and TPI-N structural unit using B3LYP/6-31G with Gaussian 09 package.

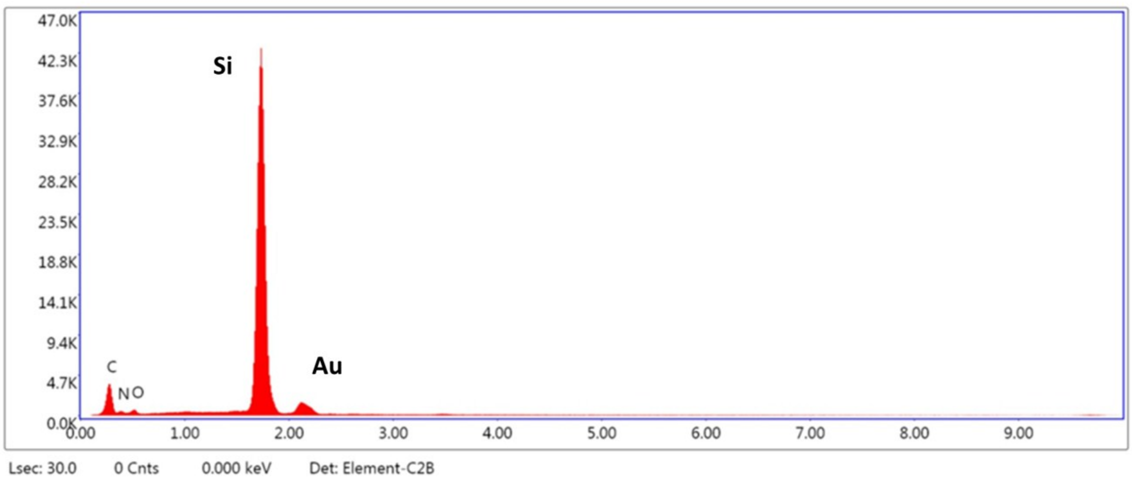

Fig. S8 EDX spectra of TPI-P-700. Standard peaks for Si and Au were observed due to Si substrate and gold coating respectively.

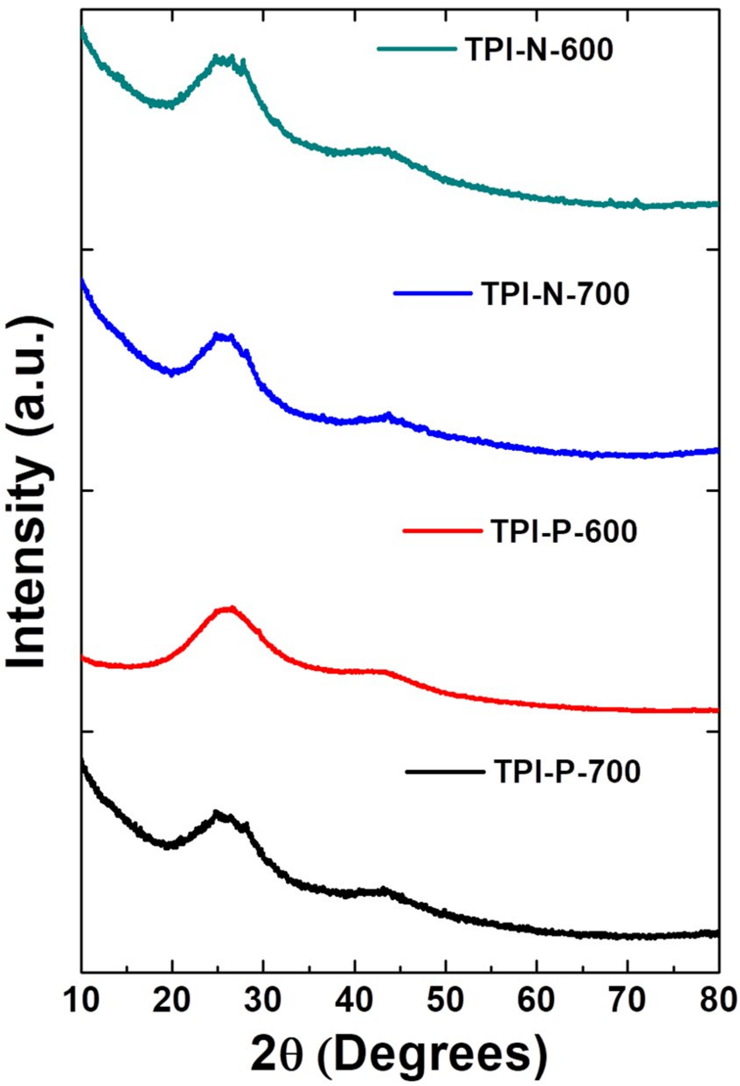

Fig. S9 Powder X-ray diffraction patterns of TPI-P-X/TPI-N-X.

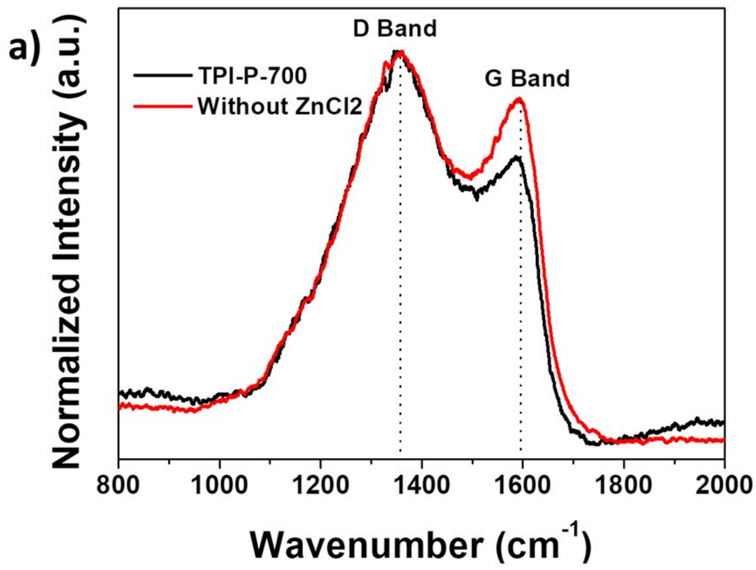

Fig. S10 Raman spectra of TPI-P precursor carbonized without $ZnCl_2$ and TPI-P-700.

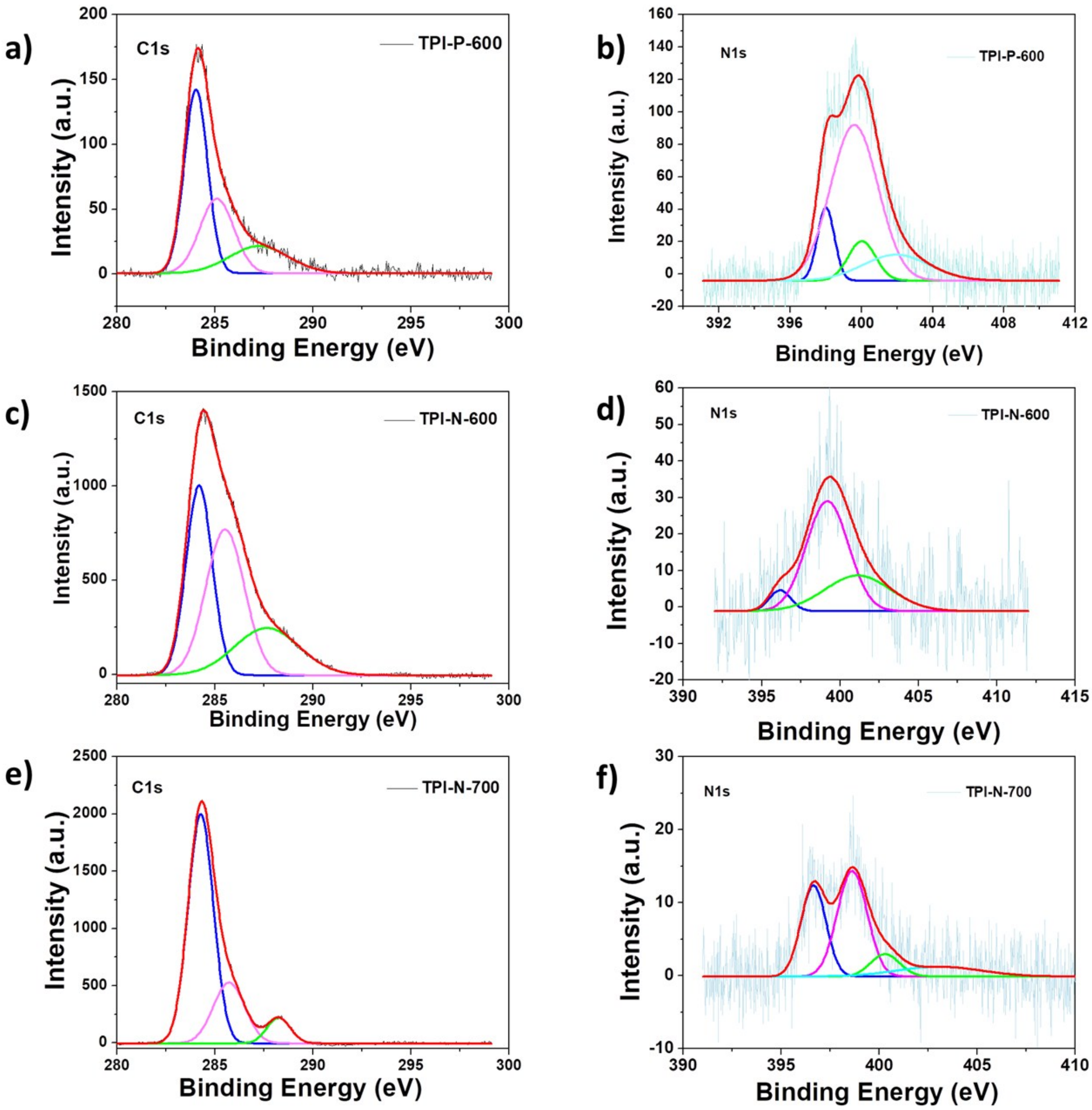

Fig. S11 Deconvoluted C1s and N1s spectra of (a, b) TPI-P-600; (c, d) TPI-N-600 and (e, f) TPI-N-700.

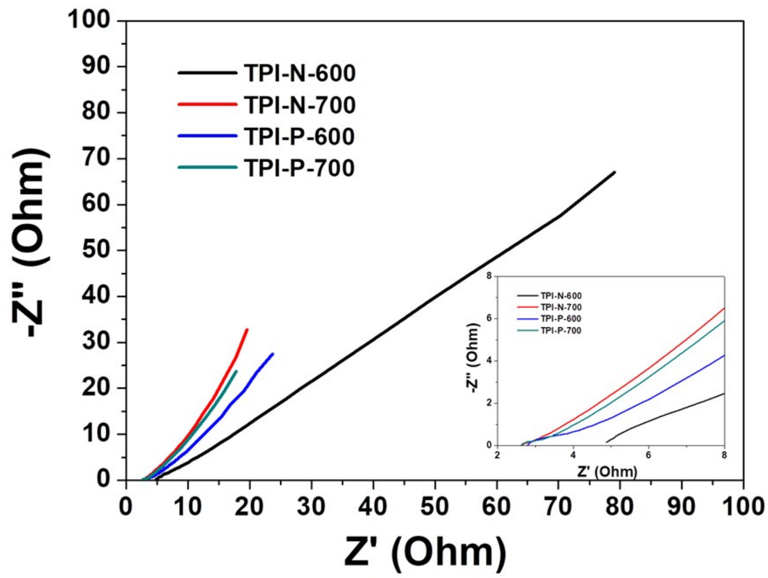

Fig. S12 Nyquist plots of N-doped porous carbon materials.

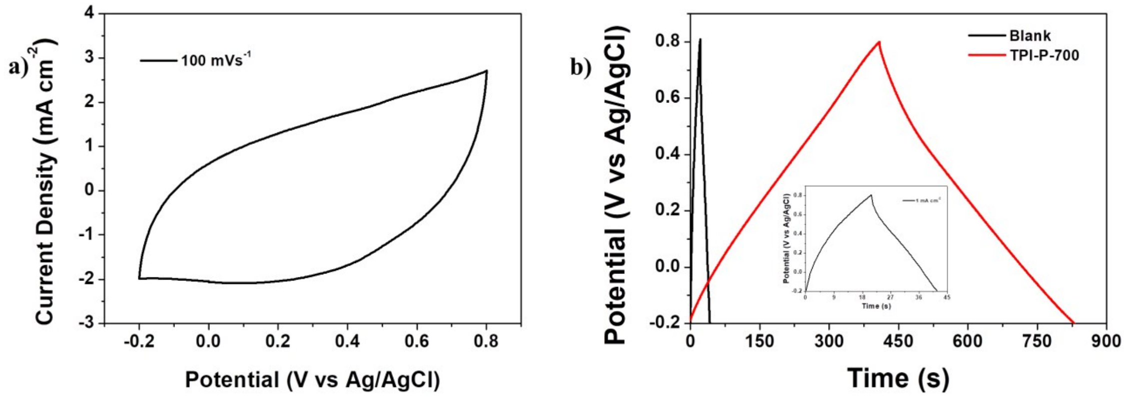

Fig. S13 a) CV curve of blank graphite sheet at 100 mV s^{-1} and b) GCD curve of graphite sheet and TPI-P-700 at 1 mA cm^{-2} in 1 M H_2SO_4 electrolyte (three electrode systems).

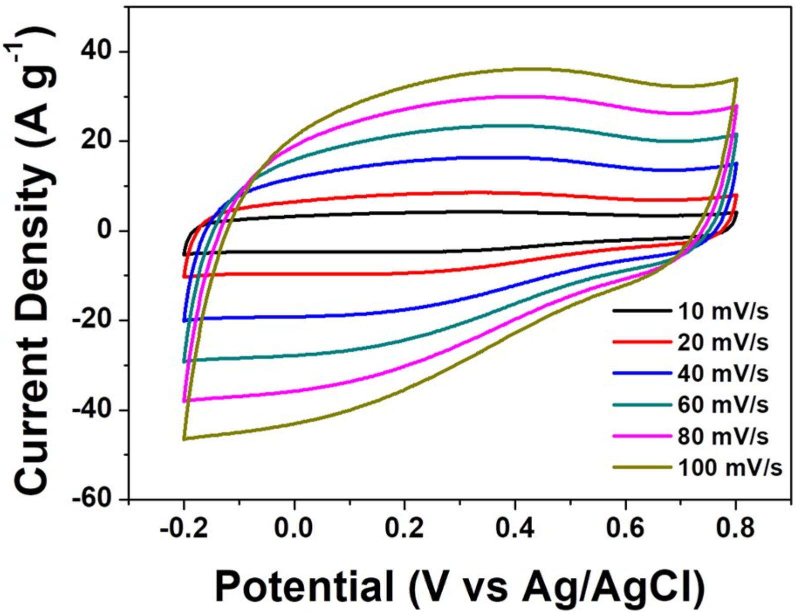

Fig. S14 CV curves of TPI-P-700 at higher rates in three electrode system.

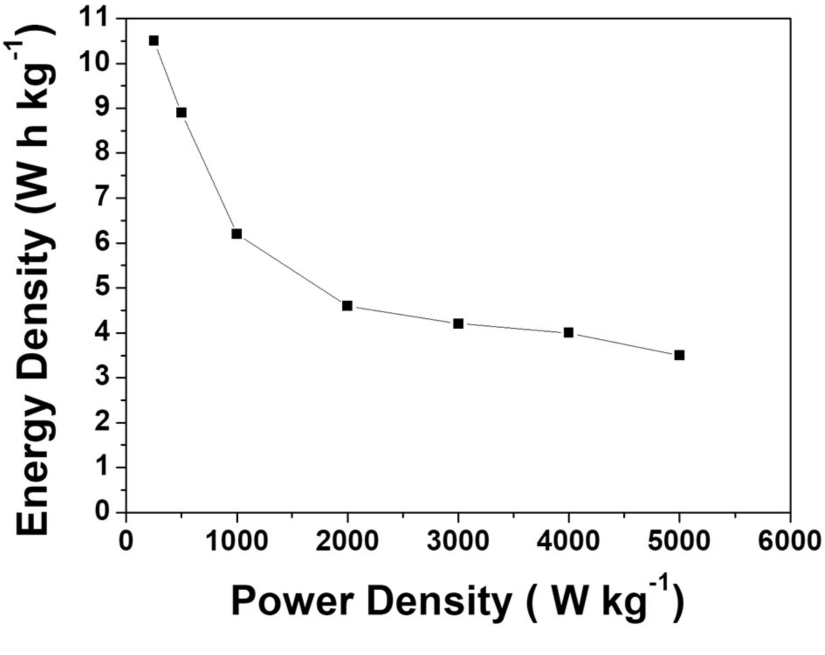

Fig. S15 Ragone plot of TPI-P-700 based symmetric supercapacitor.

Table S2 Comparative table of specific capacitance of porous carbon obtained from various metal-free precursors.

Active Material	Electrolyte	Specific Capacitance (F g^{-1})	Current density / Scan rate	Reference
Polypyrrole derived 3D hierarchical porous carbon	6 M KOH	318.2	0.5 A g^{-1}	[1]
Bagasse derived porous carbon aerogel	6 M KOH	268.4	2.0 mV s^{-1}	[2]
Lignin derived nanoporous carbon	1 M H_2SO_4	91.0	0.5 A g^{-1}	[3]
Nanocellulose derived porous carbon aerogel	6 M KOH	302.0	0.5 A g^{-1}	[4]
2D porous carbon nanosheet	6 M KOH	216.0	0.2 A g^{-1}	[5]
N-doped porous carbon capsules	1 M H_2SO_4	240.0	0.1 A g^{-1}	[6]
Biomass derived 3D hierarchical porous carbon	6 M KOH	356.0	1.0 A g^{-1}	[7]
Chitosan/PEG blend derived N-doped porous carbon	1 M H_2SO_4	356.0	1.0 A g^{-1}	[8]
Graphene like porous carbon nanosheets	6 M KOH	294.0	1.0 A g^{-1}	[9]
N-doped microporous carbon nanosphere	1 M H_2SO_4	373.0	0.2 A g^{-1}	[10]
Heteroatom-doped porous carbon	6 M KOH	416.0	0.5 A g^{-1}	[11]
Lignin derived activated carbon fibers	6 M KOH	344.0	10.0 mV s^{-1}	[12]
Cellulose derived grapheme like porous carbon sheet	6 M KOH	353.0	1.0 A g^{-1}	[13]
TPI framework derived heteroatom doped porous carbon	1 M H_2SO_4	423.0	1.0 A g^{-1}	This work

References

1. L. Qie, W. Chen, H. Xu, X. Xiong, Y. Jiang, F. Zou, X. Hu, Y. Xin, Z. Zhang and Y. Huang, *Energy Environ. Sci.*, 2013, **6**, 2497-2504.
2. P. Hao, Z. Zhao, J. Tian, H. Li, Y. Sang, G. Yu, H. Cai, H. Liu, C. P. Wong and A. Umar, *Nanoscale*, 2014, **6**, 12120-12129.
3. J.-W. Jeon, L. Zhang, J. L. Lutkenhaus, D. D. Laskar, J. P. Lemmon, D. Choi, M. I. Nandasiri, A. Hashmi, J. Xu, R. K. Motkuri, C. A. Fernandez, J. Liu, M. P. Tucker, P. B. McGrail, B. Yang and S. K. Nune, *ChemSusChem*, 2015, **8**, 428-432.
4. G. Zu, J. Shen, L. Zou, F. Wang, X. Wang, Y. Zhang and X. Yao, *Carbon*, 2016, **99**, 203-211.
5. K. Yuan, T. Hu, Y. Xu, R. Graf, G. Brunklaus, M. Forster, Y. Chen and U. Scherf, *ChemElectroChem*, 2016, **3**, 822-828.
6. G. A. Ferrero, A. B. Fuertes and M. Sevilla, *J. Mater. Chem. A*, 2015, **3**, 2914-2923.
7. S. Song, F. Ma, G. Wu, D. Ma, W. Geng and J. Wan, *J. Mater. Chem. A*, 2015, **3**, 18154-18162.
8. Y. Ba, W. Pan, S. Pi, Y. Zhao and L. Mi, *RSC Adv.*, 2018, **8**, 7072-7079.
9. B. Liu, M. Yang, H. Chen, Y. Liu, D. Yang and H. Li, *J. Power Sources*, 2018, **397**, 1-10.

10. C. Kim, K. Kim and J. H. Moon, *Sci. Rep.*, 2017, **7**, 14400.
11. T. Wei, Q. Zhang, X. Wei, Y. Gao and H. Li, *Sci. Rep.*, 2016, **6**, 22646.
12. S. Hu, S. Zhang, N. Pan and Y.-L. Hsieh, *J. Power Sources*, 2014, **270**, 106-112.
13. R.-J. Mo, Y. Zhao, M.-M. Zhao, M. Wu, C. Wang, J.-P. Li, S. Kuga and Y. Huang, *Chem. Eng. J.*, 2018, **346**, 104-112.